Ocean Sci., 12, 233–241, 2016
www.ocean-sci.net/12/233/2016/
doi:10.5194/os-12-233-2016

Ocean Science Open Access EGU

Long-term variability of the southern Adriatic circulation in relation to North Atlantic Oscillation

L. Shabrang, M. Menna, C. Pizzi, H. Lavigne, G. Civitarese, and M. Gačić

OGS – Istituto Nazionale di Oceanografia e di Geofisica Sperimentale, Trieste, Italy

Correspondence to: L. Shabrang (lshabrang@ogs.trieste.it)

Received: 15 January 2015 – Published in Ocean Sci. Discuss.: 10 February 2015
Revised: 11 January 2016 – Accepted: 15 January 2016 – Published: 12 February 2016

Abstract. The interannual variability of the South Adriatic Gyre and its relation to the wind vorticity and the large-scale climatic pattern (North Atlantic Oscillation – NAO) was studied using the time series of satellite altimetric data and ocean surface wind products. The cyclonic circulation observed in the southern Adriatic area was partly sustained by the local wind forcing, as suggested by the positive correlation between the rate of change of the current vorticity and the wind-stress vorticity. Nevertheless, the influence of vorticity advection from the adjacent area (northern Ionian Sea) cannot be ignored and it is more significant during the anticyclonic phase of Adriatic–Ionian Bimodal Oscillation System. The geostrophic current vorticities of the southern Adriatic and northern Ionian seas are correlated with a time lag of 14 months, which approximately corresponds to an advection speed of $\sim 1\,\mathrm{cm\,s^{-1}}$. The different wind patterns observed during two NAO phases in the winter revealed a stronger positive vorticity during the negative NAO phase. Conversely, during the wintertime positive NAO phase the wind vorticity is characterized by lower positive or slightly negative values. Despite a statistically significant negative correlation between the NAO index and the wind vorticity, no unequivocal relationship between large climatic system and the interannual variability of the South Adriatic Gyre intensity was found due to additional effects of the vorticity advection from the Ionian. This can be explained by the fact that the Ionian circulation mode does not depend on the NAO variations. Therefore, the main result of this study is that the interannual variability of the southern Adriatic cyclonic circulation is a result of the combined influence of the vorticity advection from the Ionian and the local wind-curl effect.

1 Introduction

The Adriatic Sea is a source of the Adriatic Dense Water (AdDW), the main component of the Eastern Mediterranean Dense Water (EMDW). The dense water formation in the Adriatic Sea takes place both in the northern Adriatic shelf area (Hendershott and Rizzoli, 1976) and in the South Adriatic Pit (SAP), in the centre of the permanent topographically trapped South Adriatic Gyre (SAG), through two different processes. In the northern Adriatic, the dense water is formed over the large northern shelf area through winter cooling and mixing, while in the southern Adriatic the dense water is formed via open-ocean convection mechanism (Gačić et al., 2002; Manca et al., 2002). These processes occur under the action of cold and severe northerly winds, more specifically the ENE or NE bora wind associated with the persistent synoptic condition and orographic configuration (Grisogono and Belušić, 2009). Major contribution to the outflowing AdDW comes from the water formed in the SAP ($\sim 90\,\%$; Vilibić and Orlić, 2001), and it presumably varies on interannual scale (Mihanović et al., 2013). The estimated total average rate of the dense water formation/outflow from the Adriatic is 0.3 Sv (1 sverdrup (Sv) $= 1\,000\,000\,\mathrm{m^3\,s^{-1}}$; Lascaratos, 1993). Obviously, this estimate is an average value and the formation rate is subject to pronounced interannual and decadal variability. Decadal variability is presumably linked to the buoyancy variations related to the import of intermediate and surface waters of varying salinity from the Ionian as associated with Adriatic–Ionian Bimodal Oscillating System (BiOS; Gačić et al., 2011). On the other hand, interannual variability of the dense water formation rate is due to a variety of factors such as surface buoyancy losses, wind forced preconditioning of surface layer density through doming of isopycnals and advective changes in density via

variations in the near-surface temperature and salinity (Josey et al., 2011). Preconditioning depends also as we will show here on the intensity of the SAG due to the local wind vorticity input and the vorticity advection from the Ionian. Variations in the strength of the SAG result in changes of the vertical distribution of isopycnals and in general in changes of the doming shape of the physical and biogeochemical interfaces.

The aim of this paper is to study the interannual variability of the SAG intensity, i.e. the vorticity of the flow field in the southern Adriatic, to relate it to the vorticity inputs (from wind and advection), and then possibly to large-scale climatic regimes (North Atlantic Oscillation (NAO) index will be considered).

2 Data and methods

The wind products used in this study were the Cross-Calibrated Multi-Platform (CCMP) ocean surface wind velocity, downloaded from the NASA Physical Oceanography DAAC (https://podaac.jpl.nasa.gov/) for the period July 1987–December 2011 (Atlas et al., 2009). These products were created using a variational analysis method to combine wind measurements derived from several satellite scatterometers and microwave radiometers. The CCMP six-hourly gridded analyses (level 3.0, first-look version 1.1, resolution of 25 km) were used to quantify the vertical component of the wind-stress curl $[\mathrm{curl}\tau]_z$ over the Mediterranean Sea:

$$[\mathrm{curl}\tau]_z = \frac{\partial \tau_y}{\partial x} - \frac{\partial \tau_x}{\partial y}; \left(\tau_x, \tau_y\right) = \rho C_\mathrm{D}\left(u_w, v_w\right) U_{10}, \qquad (1)$$

where (τ_x, τ_y) are the wind-stress components, $\rho(1.22\,\mathrm{kg\,m^{-3}})$ is the density of air, (u_w, v_w) and U_{10} are the components and the magnitude of the wind speed at 10 m, respectively, and C_D is the drag coefficient which has been obtained according to Yelland and Taylor (1996).

$$\begin{aligned} C_\mathrm{D} &= 10^{-3} \quad |U_{10}| \le 3\frac{m}{s} \\ C_\mathrm{D} &= (0.29 + \frac{3.1}{U_{10}} + \frac{7.7}{U_{10}^2}) \times 10^{-3} \quad 3\frac{m}{s} \le |U_{10}| \le 6\frac{m}{s} \\ C_\mathrm{D} &= (0.6 + 0.07U_{10}) \times 10^{-3} \quad 6\frac{m}{s} \le |U_{10}| \le 26\frac{m}{s} \end{aligned} \qquad (2)$$

The six-hourly wind-stress curl estimated from Eq. (1) was firstly time-averaged over monthly periods and finally spatially averaged in the SAG (the upper black box in Fig. 1).

The vorticity associated with the surface geostrophic circulation in the SAG and in the northern Ionian was estimated using the gridded (1/8° Mercator projection grid) Ssalto/Duacs weekly multi-mission delayed time (quality controlled) products from AVISO (SSALTO/DUACS users handbook 2014). Absolute geostrophic velocity (AGV) data, derived from the satellite absolute dynamic topography (ADT) through geostrophic balance equations, were downloaded for the 1992–2014 period. The ADT is the sum of sea level anomaly and synthetic mean dynamic topography, estimated by Rio et al. (2014), over the 1993–2012 period. The delayed time product used in this work was based on pairs of satellites (Jason-2–Altika or Jason-2–CryoSat or Jason-2–Envisat or Jason-1–Envisat or TOPEX-Poseidon–ERS) with the same ground track. This data series was homogeneous all along the available time period, thanks to a stable sampling. The relative vorticity (ζ) of the AGV data was evaluated as the vertical component of the velocity field curl (Pedlosky, 1987):

$$\zeta = \frac{\partial v_g}{\partial x} - \frac{\partial u_g}{\partial y}, \qquad (3)$$

where u_g and v_g are the components of the AGV.

Monthly means of the geostrophic current vorticity fields were spatially averaged in the region of the SAG and in the

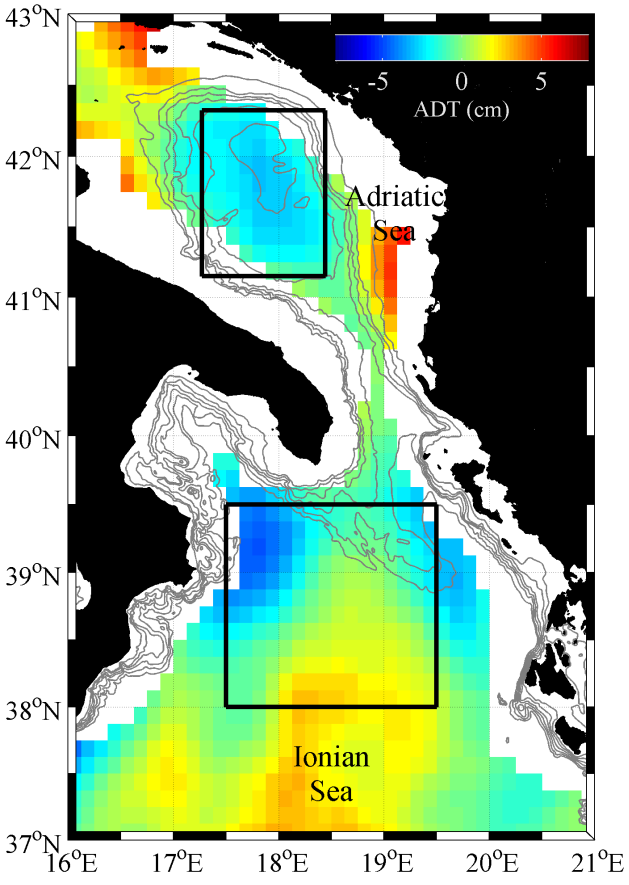

Figure 1. Geography of the southern Adriatic and northern Ionian seas. The black squares show the areas used to estimate the time series in Fig. 2. The grey contours indicate the isobaths between 200 and 1200 m with the 200 m line space. Colours show the mean altimetry pattern in the period October 1992–December 2013; altimetry grid points located within 50 km from the coast have been deleted. The Adriatic square includes 81 altimetry measurement points; the Ionian square includes 232 altimetry measurement points.

northern Ionian (areas of averaging are shown in Fig. 1). Time series of these spatially averaged parameters were filtered using a 13-month moving average, in order to remove the seasonal and intra-annual variations and focus on the interannual fluctuations. The low-pass procedure consists of a zero-phase forward and backward digital infinite impulse response filtering, with a symmetric Hanning window (Yan et al., 2004) of 13 points (months).

The vorticity equation was analysed in order to evaluate the importance of various sources of current vorticity. Following Ezer and Mellor (1994) and Schwab and Beletsky (2003), current vorticity equation can be written as

$$\frac{\partial \zeta}{\partial t} = -\mathrm{curl}(\frac{A}{D}) - \mathrm{div}(fv) - \frac{1}{\rho_0}\mathrm{curl}(\frac{1}{D}\nabla\Phi) + \mathrm{curl}(\frac{\tau_s}{\rho_0 D}) - \mathrm{curl}(\frac{\tau_b}{\rho_0 D}), \quad (4)$$

where ζ is current vorticity, A is advection and diffusion, D is total water depth, ρ_0 is the reference density, Φ is the potential energy, f is Coriolis parameter, v is current velocity, and τ_s and τ_b are wind stress and bottom stress, respectively. Since we assume the predominance of the barotropic flow, the internal pressure gradient (the third term on the right) can be ignored. We also neglect the bottom stress.

If we separate the current velocity into geostrophic (V_g) and ageostrophic (V_a) parts and consider the non-divergence of the geostrophic current, we will have

$$V = V_g + V_a; \quad \zeta = \zeta_g + \zeta_a \quad (5)$$

$$\mathrm{div}(fV) = f\left(\frac{\partial u_a}{\partial x} + \frac{\partial v_a}{\partial y}\right) = \frac{f}{D}\left(\frac{\mathrm{d}h}{\mathrm{d}t}\right), \quad (6)$$

Replacing Eqs. (5) and (6) in Eq. (4) and neglecting the diffusion A as well as bottom stress and divergence ($\frac{f}{D}(\frac{\mathrm{d}h}{\mathrm{d}t})$, which is 2 orders of magnitude smaller than rate of change of the vorticity) implies

$$\frac{\partial(\zeta_g + \zeta_a)}{\partial t} = -(V_g + V_a)\cdot\nabla(\zeta_g + \zeta_a) + \frac{1}{\rho D}\mathrm{curl}(\tau_s). \quad (7)$$

Since $\frac{|V_a|}{|V_g|} = \frac{|\zeta_a|}{|\zeta_g|} \sim O(Ro) = O(\frac{U}{fL}) = 10^{-2}$ ($U \sim 10^{-1}\frac{m}{s}$, $L \sim 10^5$ m, $f \sim 10^{-4}\,\mathrm{s}^{-1}$), the ageostrophic parts vanish and finally we obtain the current vorticity equation:

$$\frac{\partial \zeta_g}{\partial t} = -V_g\cdot\nabla(\zeta_g) + \frac{1}{\rho D}\mathrm{curl}(\tau_s), \quad (8)$$

which shows that the variation of the geostrophic current vorticity can be explained in terms of the wind-stress vorticity as well as vorticity advection from the neighbouring areas.

The monthly NAO index used in this work was obtained from the National Weather Service, Climate Prediction Center of NOAA (National Oceanic and Atmospheric Administration). The procedures used to identify the NAO index was the rotated principal component analysis (RPCA, Barnston and Livezey, 1987). The RPCA procedure is superior to grid-point-based analyses, typically determined from one-point correlation maps, in that the teleconnection patterns in the RPCA approach are identified based on the entire flow field, and not just from height anomalies at selected locations (http://www.cpc.ncep.noaa.gov/data/teledoc/nao.shtml).

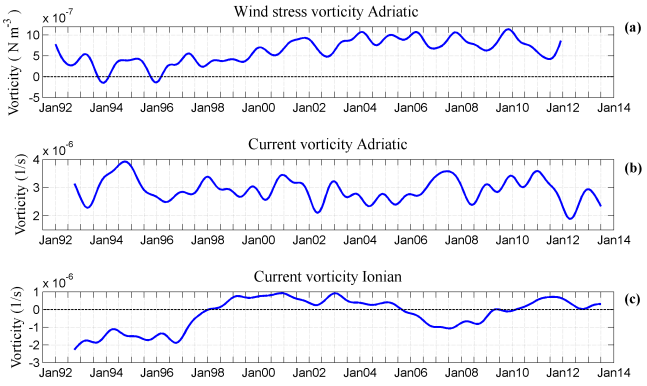

Figure 2. Time series of the spatially averaged, low-pass filtered (13 months) wind-stress vorticity **(a)** and current vorticity **(b)** in the Adriatic Sea, computed over the domain denoted in Fig. 1. Time series of the low-pass filtered current vorticity in the Ionian Sea **(c)** spatially averaged over the domain presented in Fig. 1.

3 Results and discussion

Calculations of the spatially averaged current vorticity (Fig. 2b) show that the southern Adriatic was characterized, as expected, by a permanent positive vorticity since the SAG is a cyclonic circulation feature. Nevertheless, prominent interannual or decadal variability was present in the time series (Fig. 2). The interannual variability prevailed also in the wind-stress curl (Fig. 2a), while decadal variability was prevalent in the vorticity field of the northern Ionian (Fig. 2c). In fact, the vorticity field in the northern Ionian is mainly subject to decadal variability due to BiOS (Gačić et al., 2010) as opposed to the Adriatic current vorticity and the wind-stress curl. The vorticity of the wind field was positive for the major part of the record with only short periods of negative values (Fig. 2a).

Considering the flow vorticity Eq. (8), interannual variability of the intensity of the geostrophic cyclonic circulation in the southern Adriatic can be only partly explained in terms of the local wind vorticity input, this last one being prevalently positive. Thus in addition to the local wind-curl effect, the vorticity advection from adjacent area should be taken into consideration.

First to estimate the importance of the local input in the vorticity equation, we compared the time series of the current vorticity tendency with the curl of the wind stress over the winter months, from January to March (hereafter we refer to this time period as JFM), calculating the linear correlation coefficient in each data point of the study domain. Winter-

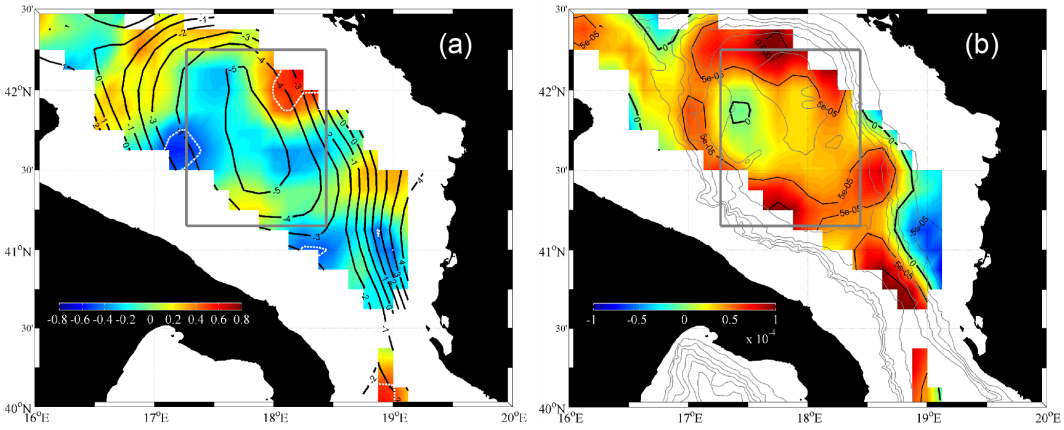

Figure 3. Spatial distribution of the correlation coefficient between the JFM time derivative of the vorticity and the wind-stress curl for the period 1993–2011 (colours). Black bold contours outline the 20-year average of the JFM sea level height (cm), and the white dotted lines indicate the level of the 95 % significance **(a)**; spatial distribution of the average of the JFM geostrophic current vorticity (colours and the black lines). The grey contours indicate the isobaths between 200and 1200 m with the 200 m line space **(b)**. The grey squares show the areas used to estimate the time series in Fig. 2; altimetry grid points located within 50 km from the coast have been deleted.

time values were chosen because strong air–sea interaction (wind forcing and possible relationship to NAO) occurs during the winter months when deep convection takes place. As it follows from the vorticity equation (Eq. 8) the vorticity tendency and the wind-stress curl should be positively correlated.

The spatial distribution of the correlation coefficients over the study area shows a rather patchy pattern. The area of the significant positive correlation ($r \geq 0.6; s \geq 0.95$) northeast of the gyre (see Fig. 3a) coincides rather well with the maximum of the current vorticity average (Fig. 3b), and there probably the main wind vorticity input takes place. This suggests that in a limited area the Ekman suction controls the strength of the SAG determining the strength of the gyre. In the centre of the gyre, the correlation diminishes probably due to the generally small values of the current vorticity. In addition, some small-scale features characterized by the negative correlation are present west and south of the gyre, which can be explained in terms of the vortex stretching due to strong bathymetric features. The significant negative correlation ($r \leq -0.5; s \geq 0.95$) west of the gyre (around 17°15′ E and 41°40′ N) is probably due to the topographic anomaly near the Bari Canyon (Cushman-Roisin et al., 2001), which may generate strong ageostrophic divergence. Therefore, in accordance with the quasi-geostrophic equation of the vorticity conservation, the mechanism partially responsible for the variations of the current vorticity is the wind-stress curl acting in a limited area of the SAG. The fact that direct forcing from the wind-stress curl could be an important mechanism determining the vorticity of the mean circulation pattern was also evidenced in some large lakes (Schwab and Beletsky, 2003).

The second term that may contribute to the vorticity tendency in the SAP is the advection term. In order to study to what extent the vorticity advection from the Ionian plays a role in controlling the curl of the flow in the southern Adriatic, we first calculated the lagged correlation between the spatially averaged vorticity in the northern Ionian and southern Adriatic (figure not shown). The correlation between the low-pass Adriatic and Ionian flow vorticities reached maximum ($r \sim 0.4$) for the Adriatic vorticity lagging the Ionian one by about 14 months. It should be mentioned that by decreasing the degrees of freedom of the time series from ~ 240 to ~ 20 due to the filtering procedure, the level of confidence of the correlation decreases. In other words, according to the standard t table (e.g. Snedecor and Cochran, 1980) the correlation coefficients must exceed 0.423 to be significant at 95 % confidence level. Furthermore, as far as the estimates of the time lag are concerned the same value (14 months) was obtained using either unfiltered data or data filtered with different window lengths (figure not shown). This time lag corresponds approximately to the advection speed of 1 cm s^{-1}, a rather reasonable value. Then, in order to determine with more precision the vorticity source area in the northern Ionian Sea, the 14-month lag correlations between the spatial average of the low-passed current vorticity in the SAG (the upper domain in the Fig. 4a) and average vorticity in smaller domains ($0.25° \times 0.25°$) in the northern Ionian were calculated (see Fig. 4a). All over the area of the northern Ionian the correlation coefficients are positive with a maximum located in the northern part of North Ionian Gyre (NIG) (around 18°30′ E, 39°30′ N) where the horizontal shear is the strongest during the anticyclonic mode of BiOS (Gačić et al., 2011). Afterwards, the lag correlation between the filtered time series of the mean vorticities in the SAG and the area where maximum correlation between SAG and Ionian was evidenced (the small polygon located in 18°30′ E, 39°30′ N in the Fig. 4a) was calculated. The maximum correlation co-

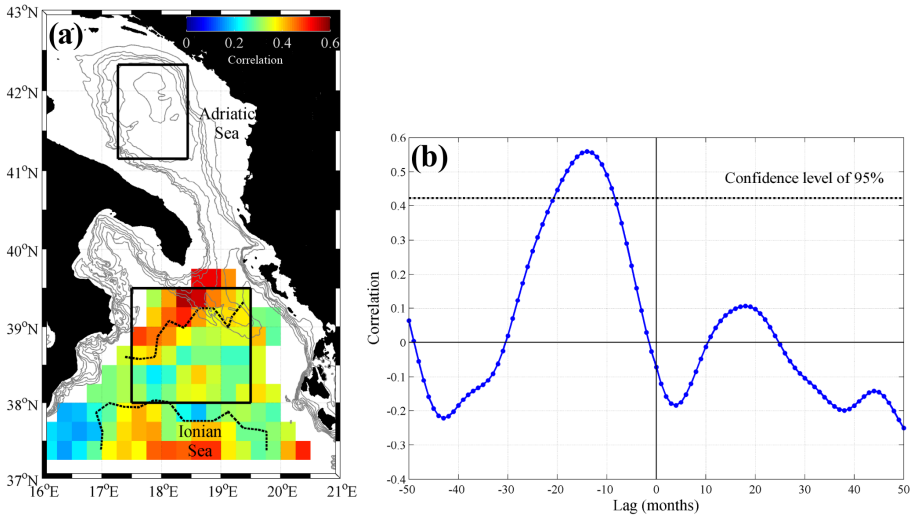

Figure 4. Correlation between the time series of the spatially averaged low-pass current vorticity in the Adriatic and 0.25° × 0.25° domains in the Ionian for the 14-month time lag **(a)**; lagged correlation between Adriatic and Ionian spatially averaged vorticities. For the Adriatic the averaging domain is the upper polygon while for the northern Ionian the averaging domain corresponds to the area (0.25° × 0.25°) with the maximum correlation **(b)**; the black polygons show the areas used to estimate the time series in Fig. 2; the black dotted lines indicate the level of confidence of 95 %.

efficient ($r \sim 0.56$) with the higher level of confidence (99 %) is evidenced again for the time lag = 14 months (see Fig. 4b), which confirms the impact of the vorticity in this area on the SAG circulation. Although the estimated correlation coefficient is relatively large, the relation between vorticities in these two areas is not visible inspecting the time series (see Fig. 2b and c). This can be explained by the fact that, according to Eq. (8), vorticity advection only partly determines the variation of the circulation in the SAP while the additional contribution comes from the wind input. Therefore, the influence of Ionian circulation to the current vorticity of the SAP cannot be clear in the visual examination of the vorticity time series. More specifically, the advection term is not equally important in all situations; in 1997, the reversal of the northern Ionian circulation took place from anticyclonic to cyclonic mode (Larnicol et al., 2002; Pujol and Larnicol, 2005). The continuous reduction of the current vorticity term between 1995 and 1999 (see Fig. 5a) is due to this circulation transition. The subsequent passage from cyclonic to anticyclonic circulation in the northern Ionian Sea occurred in 2006 (Gačić et al., 2010), which has as a consequence an increase of the relative importance of the advection term. Therefore, when the Ionian circulation is in the anticyclonic phase the advection term is more important than in the cyclonic phase. In the former case, the advection term is proportional to the sum of the Ionian and Adriatic vorticities while in the latter case the advection term is proportional to the difference between the two vorticities (see Eq. 8). In order to examine the relative importance of the advection term in each mode of BiOS, we compare the vorticity tendency with the advection term in Eq. (8):

$$\frac{\partial \xi_g}{\partial t} = -V_g \cdot \nabla(\xi_g) + A, \tag{9}$$

where A is the wind-stress vorticity. Then, Eq. (9) expressed in terms of the finite differences becomes

$$\frac{\Delta \xi_g}{\Delta t} = -V \times \frac{\Delta \xi_g}{\Delta x} + A. \tag{10}$$

Then considering only the advection term, we obtain

$$\xi_{g-\mathrm{SAG}}(t+1) - \xi_{g-\mathrm{SAG}}(t-1) \propto C \times \left(\xi_{g-\mathrm{SAG}}(t) - \xi_{g-\mathrm{NIG}}(t)\right), \tag{11}$$

in which $\xi_{g-\mathrm{SAG}}$ and $\xi_{g-\mathrm{NIG}}$ are the spatial average of the curl of geostrophic current in SAG and in the small polygon in the NIG located around 18°30′ E and 39°30′ N, respectively. Furthermore, we assume that $C = \left|-V\frac{\Delta t}{\Delta x}\right|$ is a constant obtained from the time step, the distance between the Ionian vorticity source area and the SAP, and considering the constant advection speed.

Using Eq. (11), vorticity tendency in the SAP was compared to the difference of the vorticities between the SAP and the northern portion of NIG plotting the scatter diagram for the periods associated with the cyclonic (red) and anticyclonic (blue) modes of BiOS (Fig. 5b). The figure reveals rather satisfactory linear relation between two terms during the anticyclonic phase, when the vorticity advection becomes more important. Conversely, in the cyclonic mode of the Ionian circulation, the difference of the vorticities in the SAP and NIG is smaller and the advection does not have the significant influence on the vorticity variations in the SAG. In

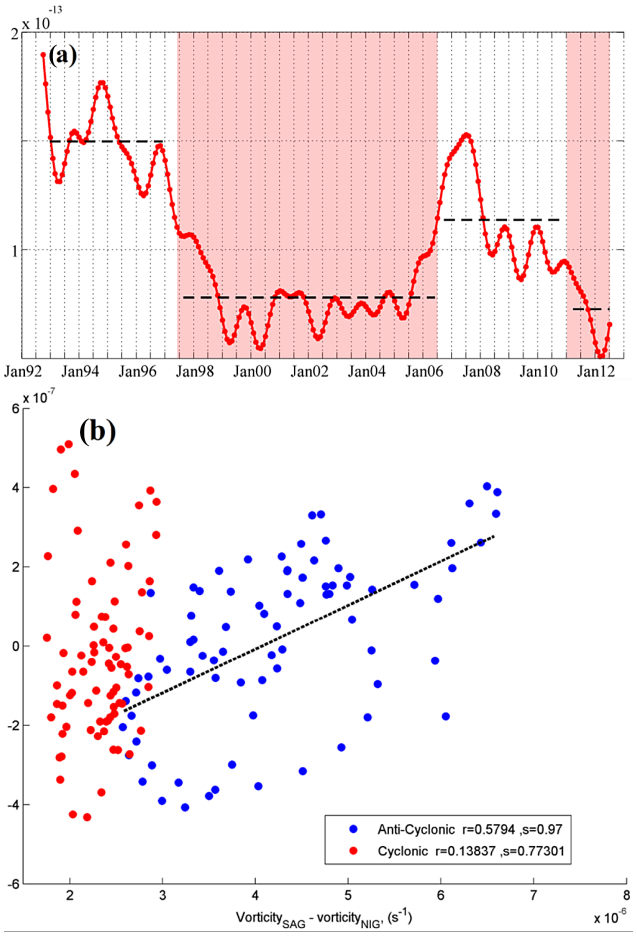

Figure 5. Time series of the low-pass (13 months) current vorticity advection from the northern Ionian Sea to the southern Adriatic Sea. Areas shaded in red correspond to the time periods characterized by cyclonic circulation mode, and the dashed lines show the average values of the advection over each cyclonic/anticyclonic periods **(a)**; scatter plot of the vorticity tendency (in finite differences) in the SAP (Fig. 2b) and the difference of vorticities in the Adriatic and the northern area of NIG during the cyclonic (red circles) and anticyclonic (blue circles) modes of BiOS **(b)**.

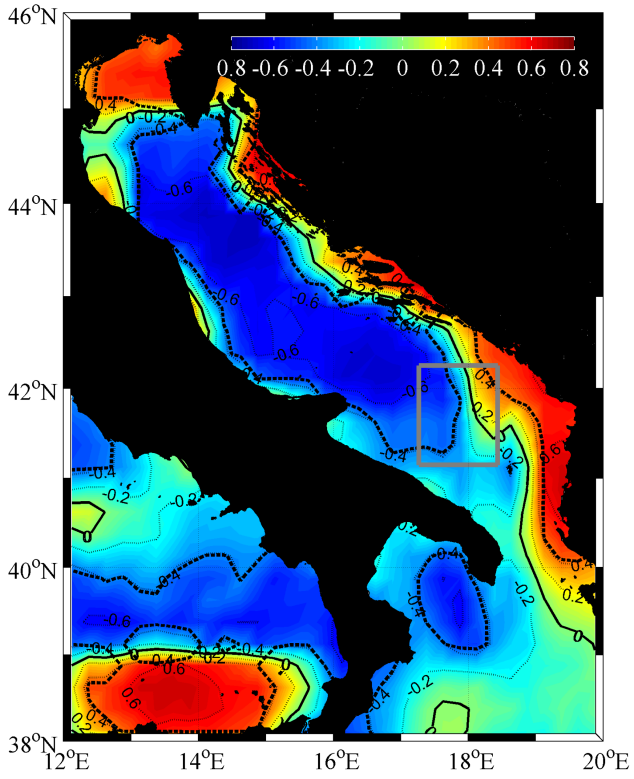

Figure 6. Spatial distribution of the correlation coefficient of the JFM NAO index and wind-stress vorticity, 1988–2011 (coloured area and dotted lines). The bold solid and dashed lines indicate the 0 correlation and the 95 % significance isoline, respectively. The square shows the area used to estimate the time series in Fig. 2.

addition, from the calculated linear regression between two terms of Eq. (11), we obtained the advection speed of about 0.8 cm s^{-1}, which is rather consistent with the estimate obtained from the lagged correlation between the NIG and SAP vorticities.

Therefore, the local current vorticity input prevailed in the period 1997–2006 when the Ionian was in the cyclonic phase and the advection term was less important. Before 1997 and after 2006 the Ionian was characterized by the anticyclonic circulation mode, and the vorticity advection term was more important.

In order to relate the interannual variability of the wind-stress curl (one of the important factors affecting the variation of the strength of the gyre according to Eq. 8) to NAO as a large climatic system, we compared time series of the wintertime NAO index with the wind-stress curl. More specifically, we calculated the correlation coefficient between the two time series in each point of the study area for the period 1988–2011 (Fig. 6). Previous research showed that the correlation between the wind speed and NAO in the Adriatic was statistically insignificant (Pirazzoli and Tomasin, 2003). Considering however the wind-stress curl, the results revealed the significant (95 %) negative correlation between the wind-stress curl and NAO for the major portion of the open Adriatic Sea: NAO index negative values were concomitant with maximum wind-stress curl, and conversely minima of the wind-stress curl were associated with NAO maximum values.

During the positive NAO phase, northwesterlies are dominant in southern Europe and Mediterranean Sea as the result of the enhancement of the Icelandic Low as well as of the Azores High. Conversely, in the negative phase, the intensification of the westerlies is observed in these regions (Jerez et al., 2013). More specifically, depending on the phase of NAO, the pressure gradient over the North Atlantic changes in the magnitude and orientation, which causes the differences in the speed and direction of winds in mid-

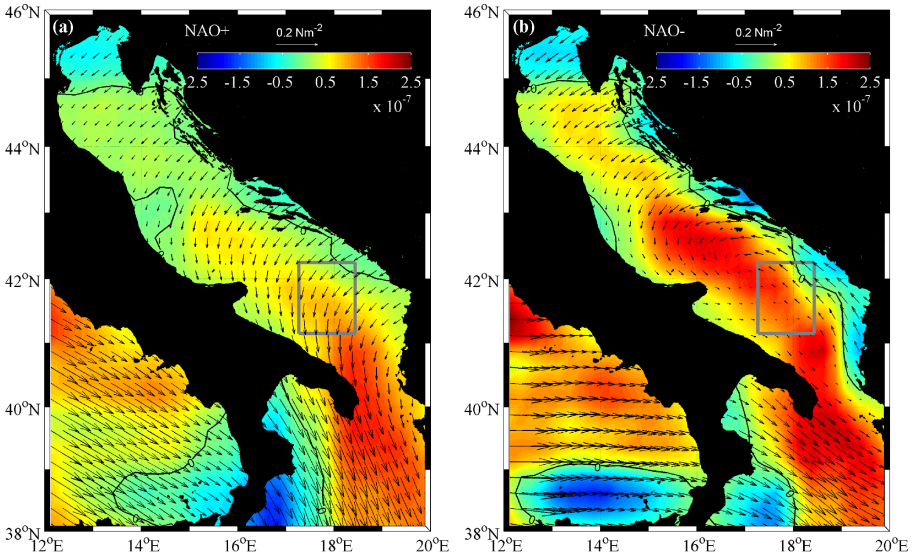

Figure 7. Spatial distribution of the mean JFM wind-stress vorticity (colours; Nm^{-3}) and wind-stress vectors (arrows; Nm^{-2}) in the positive NAO phase **(a)** and negative NAO phase **(b)**, 1988–2011. The squares show the areas used to estimate the time series in Fig. 2.

latitudes (Lamb and Peppler, 1987). In agreement with Trigo et al. (2002), the local maxima of the wind vorticity were present in the southern Adriatic Sea during both positive and negative NAO phases. The positive winter NAO indices were followed by strong northwesterly winds over the Mediterranean, which is the consequence of the intensification of the high pressure over the Mediterranean region (Fig. 7a). This configuration resulted in a rather weak low-pressure centre over the southern Adriatic and a weakening of the cyclonic vorticity. On the contrary, during the negative NAO periods rather strong northward atmospheric flow along the eastern coast of the southern Adriatic was observed, reinforcing the wind-stress curl (Fig. 7b).

Therefore, we can say that the large-scale climatic conditions associated with a positive NAO phase weaken the positive wind-stress curl, while the stronger positive wind-stress curl is related to the negative NAO index. The wind-stress curl, on its turn, affects the current vorticity tendency in the central part of the southern Adriatic however depending on the circulation mode of BiOS. In the cyclonic phase, the wind-stress curl is presumably prevailing in determining the vorticity tendency, while in the anticyclonic phase the vorticity advection term becomes important. In conclusion, due to the varying importance of the vorticity advection term, which depends on the Ionian circulation mode, it is not possible to establish an unequivocal relationship between NAO and the strength of the SAG.

4 Conclusions

Intensity of the SAG shows prominent intra-annual and interannual variability. In this paper its interannual variability was analysed using the surface geostrophic current vorticity. Local forcing is analysed considering the wind-stress curl in the area of the southern Adriatic, while advective contributions were examined to analyse the vorticity in the adjacent area, i.e. the northern Ionian. Correlation between the wintertime wind-stress curl and the geostrophic vorticity tendency reaches local maximum on the northeast of the SAG (Fig. 3a) coinciding with the maximum of the current vorticity average (Fig. 3b). We thus conclude that the current vorticity tendency can partially be explained in terms of the local wind vorticity input.

Subsequently, the moving correlation between the current vorticity in the northern Ionian, possible source area, and in the southern Adriatic shows that the vorticity variations in the Adriatic lag those in the Ionian by about 14 months (Fig. 4b). This suggests that the advection speed is about 1 $cm\,s^{-1}$. Calculating the correlation between the average current vorticity at the SAG and each small polygon of the NIG, the strongest advection signal from northern Ionian to the South Adriatic Gyre is recognized to be from the northern area of the NIG (Fig. 4a). This location coincides with the strongest horizontal shear during anticyclonic BiOS. The scatter diagram between the SAG vorticity tendency and vorticity differences between SAG and northern part of NIG reveals the stronger impact of the advection term with the speed $\sim 0.8\,cm\,s^{-1}$ (close to the previously obtained advection speed) during the anti-cyclonic mode of BiOS. It implies that the importance of the advective term in the vorticity equation depends on the BiOS circulation mode. It was revealed that in the BiOS cyclonic phase the main vorticity input into the SAG comes from the wind-stress curl although we cannot exclude completely the advection term. In the anticyclonic phase the ad-

vective vorticity input from the Ionian becomes larger and presumably more important for the overall SAG vorticity tendency than during the cyclonic phase (Fig. 5a and b). The large-scale climatic conditions were presented by the NAO index, and the wind-stress curl variations were related to them. Comparison between the NAO and the wind-stress curl shows that in both positive and negative NAO phases cyclonic atmospheric circulation is dominant, but higher vorticity in the wind field coincides with negative NAO, and conversely smaller values of the wind-stress curl are concomitant with positive NAO values (Fig. 7). This was explained in terms of the prevailing atmospheric flows over the larger Mediterranean area.

This analysis therefore suggests that, to a certain extent, the interannual variations of the strength of the SAG are associated with the large-scale climatic variations via the wind-stress curl forcing. However, due to the rather important contribution of the vorticity advection from the Ionian, characterized by the prevalent decadal variability, there is no clear evidence of a direct effect of large-scale atmospheric circulation over the NAO on the interannual variability of the intensity of the SAG.

Acknowledgements. The altimeter data were produced by SSALTO/DUACS and distributed by AVISO, with support from CNES (http://www.aviso.oceanobs.com/duacs/). We thank S. Neske for the contribution to the work during her internship stay at OGS. We express our thanks to A. Mellit for help with the statistical analysis. We acknowledge the support to H. Lavigne of the European Commission "Cofunded by the European Union under FP7-People – Co-funding of Regional, National and International Programmes, GA no. 600407" and of the RITMARE Flagship Project. The research was partially financed by the national project MedGES of the Italian Ministry of Education, University and Research.

Edited by: M. Hoppema

References

Atlas, R., Ardizzone, J. V., Hoffman, R., Jusem, J. C., and Leidner, S. M.: Cross-calibrated, multi-platform ocean surface wind velocity product (MEaSUREs Project), Guide Document, Physical Oceanography Distributed Active Archive Center (PO.DAAC), JPL, Pasadena, California, 18 May 2009, Version 1.0., 26 pp., 2009.

Barnston, A. G. and Livezey, R. E.: Classification, seasonality and persistence of low frequency atmospheric circulation patterns, Mon. Weather Rev., 115, 1083–1126, 1987.

Cushman-Roisin, B., Gačić, M., Poulain, P. M., and Artegiani, A.: physical oceanography of the Adriatic Sea; Past, present and future, 126 pp., Kluwer Academic Publishers, Dordrecht, 2001.

Ezer, T. and Mellor G. L.: Diagnostic and prognostic calculations of the North Atlantic circulation and sea level using a sigma coordinate ocean model, J. Geophys. Res., 99, 14159–14171, 1994.

Gačić, M., Civitarese, G., Miserocchi, S., Cardin, V., Crise A., and Mauri, E.: The open-ocean convention in the Southern Adriatic: a controlling mechanism of the spring phytoplankton bloom, Cont. Shelf Res., 22, 1897–1908, 2002.

Gačić, M., Eusebi Borzelli G. L., Civitarese G., Cardin V., and Yari S.: Can internal processes sustain reversals of the ocean upper circulation? The Ionian Sea example, Geophys. Res. Lett., 37, L09608, doi:10.1029/2010GL043216, 2010.

Gačić, M., Civitarese, G., Eusebi Borzelli, G. L., Kovačević, V., Poulain, P-M., Theocharis, A., Menna, M., Catucci A., and Zarokanellos, N.: On the relationship between the decadal oscillations of the Northern Ionian Sea and the salinity distributions in the Eastern Mediterranean, J. Geophys. Res., 116, C12002, doi:10.1029/2011JC007280, 2011.

Grisogono, B. and Belušić, D.: A review of recent advances in understanding the meso- and microscale properties of the severe Bora wind, Tellus A, 61, 1–16, 2009.

Hendershott, M. C. and Malanotte-Rizzoli, P.: The winter circulation of the Adriatic Sea, Deep-Sea Res., 23, 353–370, 1976.

Jerez, S., Jimenez-Guerrero, P., Montávez, J. P., and Trigo, R. M.: Impact of the North Atlantic Oscillation on European aerosol ground levels through local processes: a seasonal model-based assessment using fixed anthropogenic emissions, Atmos. Chem. Phys., 13, 11195–11207, doi:10.5194/acp-13-11195-2013, 2013.

Josey, S. A, Somot, S., and Tsimplis, M.: Impacts of atmospheric modes of variability on Mediterranean Sea surface heat exchange, J. Geophys. Res., 116, C02032, doi:10.1029/2010JC006685, 2011.

Lamb P. J. and Peppler R. A: North Atlantic Oscillation: concept and an application, B. Am. Meteorol. Soc. 68, 1218–1225, 1987.

Larnicol, G., Ayoub, N., and Le Traon, P. Y.: Major changes in Mediterranean Sea level variability from 7 years of TOPEX/Poseidon and ERS-1/2 data, J. Mar. Syst., 33–34, 63–89, doi:10.1016/S0924-7963(02)00053-2, 2002.

Lascaratos, A.: Estimation of deep and intermediate water formation rates in the Mediterranean Sea, Deep-Sea Res. PT. II, 40, 1327–1332, 1993.

Manca, B. B., Kovačević, V., Gačić, M., and Viezzoli, D.: Dense water formation in the Southern Adriatic Sea and spreading into the Ionian Sea in the period 1997–1999, J. Marine Syst., 33–34, 133–154, 2002.

Mihanović, H., Vilibić, I., Carniel, S., Tudor, M., Russo, A., Bergamasco, A., Bubić, N., Ljubešić, Z., Viličić, D., Boldrin, A., Malačič, V., Celio, M., Comici, C., and Raicich, F: Exceptional dense water formation on the Adriatic shelf in the winter of 2012, Ocean Sci., 9, 561–572, doi:10.5194/os-9-561-2013, 2013.

Pedlosky, J.: Geophysical Fluid Dynamics, 2nd ed., 710 pp., Springer, New York, 1987.

Pirazzoli, P. A. and Tomasin, A.: Recent near-surface wind changes in the Central Mediterranean and Adriatic areas, Int. J. Climatol., 23, 963–973, 2003.

Pujol, M. I. and Larnicol G.: Mediterranean Sea eddy kinetic energy variability from 11 years of altimetric data, J. Mar. Syst., 58, 121–142, doi:10.1016/j.jmarsys.2005.07.005, 2005.

Rio, M.-H., Pascual, A., Poulain, P.-M., Menna, M., Barceló, B., and Tintoré, J.: Computation of a new mean dynamic topography for the Mediterranean Sea from model outputs, altimeter measurements and oceanographic in situ data, Ocean Sci., 10, 731–744, doi:10.5194/os-10-731-2014, 2014.

Schwab, D. J. and Beletsky D.: Relative effects of wind-stress curl, topography, and stratification on large-scale circulation in Lake Michigan, J. Geophys. Res., 108, 3044, doi:10.1029/2001JC001066, 2003.

Snedecor, G. W. and Cochran, W. G.: Statistical Methods, 7th Edn. Ames: Iowa State University Press, 1980.

Trigo, R. M., Osborn, T. J., and Corte-Real, J. M.: The North Atlantic Oscillation influence on Europe: climate impacts and associated physical mechanisms, Clim. Res., 20, 9–17, 2002.

Vilibić, I. and Orlić, M.: Least-squares tracer analysis of water masses in the South Adriatic (1967–1990), Deep-Sea Res. Pt. I, 48, 2297–2330, 2001.

Yan, H., Zhong, M., and Zhu, Y.: Determination of the Degree of Freedom of Digital Filtered Time Series With an Application to the Correlation Analysis Between the Length of Day and the Southern Oscillation Index, Chin. Astron. Astrophy., 28, 120–126, 2004.

Yelland, M. and Taylor P. K.: Wind-stress measurements from the open ocean, J. Phys. Oceanogr., 26, 541–558, 1996.